J Mater Sci (2020) 55:4848–4863

Materials for life sciences

Novel protein-based bio-aerogels derived from canola seed meal

Sarah E. Fitzpatrick[1], Santanu Deb-Choudhury[2], Steve Ranford[2], and Mark P. Staiger[1,*]

[1] Department of Mechanical Engineering, University of Canterbury, Private Bag 4800, Christchurch 8140, New Zealand
[2] AgResearch Ltd., Lincoln Research Centre, Private Bag 4749, Christchurch 8140, New Zealand

Received: 8 October 2019
Accepted: 26 December 2019
Published online: 6 January 2020

ABSTRACT

Novel bio-aerogels produced via the gelation of protein extracts from canola seed meal (CSM) are described for the first time, representing a new class of advanced materials that are derived from plant-based biotechnology. The bio-aerogels were synthesised by firstly manipulating the pH of the protein solution to form a gel, followed by freeze drying to form an aerogel with an average pore size and density of 75 μm and 0.13 g cm^{-3}, respectively. The resulting protein-based structures were observed to have pores sizes down to the meso-scale. The mechanical behaviour of CSM-derived protein aerogels was investigated using static compressive testing. The average compressive elastic moduli and strength of the aerogels were 0.97 ± 0.32 MPa and 0.055 ± 0.011 MPa, respectively. The CSM-derived protein aerogels had compressive mechanical properties up to 196% of soy protein composite aerogels. The mechanical properties could also be manipulated by altering the pH and temperature during gelation. Gels held at ambient temperature during processing were revealed to have the highest elastic moduli (2.0 ± 0.6 MPa) and compressive strength (0.096 ± 0.014 MPa) at a pH of 8. In contrast, gels that were heated at 90 °C demonstrated the highest compressive modulus and strength at a pH of 10 (133% and 140%, respectively, as compared to the gel at pH 8 prepared at ambient temperature). The tunability of the mechanical properties using simple aqueous chemistry suggests this novel system of bio-aerogels has potential uses in a range of food and biopharmaceutical applications.

Introduction

Aerogels are a unique class of advanced materials that are synthesised to be highly porous, leading to a combination of ultra-low density and exceedingly high surface area [1]. An aerogel is formed when the liquid phase within the pores of a gel (inorganic or organic) is replaced with air, without significant shrinkage of the pore structure [2]. The resulting low-density structure of aerogels leads to many technologically interesting applications due to the high

Address correspondence to E-mail: mark.staiger@canterbury.ac.nz

https://doi.org/10.1007/s10853-019-04330-w

specific surface area (600–1000 $m^2 g^{-1}$ [3]) and strength (0.6–2.2 MPa $(kg\ m^{-3})^{-1}$ [4]) of aerogels. Most aerogel properties are a direct consequence of the micro- and meso-porosity of the gels, where pores are classified according to size (macro-pores are > 50 nm, meso-pores 2–50 nm, and micro-pores < 2 nm in width).

Various organic materials (e.g. synthetic or bio-based polymers, and proteins) have been shown to form an aerogel or aerogel-like structure [5–7]. Recently, the unique properties of both bio-based polymers (biodegradability, biocompatibility, bioactivity, etc.) and aerogels have prompted investigation into potential synergistic effects with the development of bio-aerogels. For example, biocompatible aerogels with specific porosities are effective cell scaffolds in tissue engineering applications [8]. Other bio-specific applications where biopolymers offer an advantage due to digestibility include drug delivery [9] and food science [10]. Aerogels produced from more sustainable precursors are also a strong driver in this field [7]. Bio-aerogels based on polysaccharides are a popular choice due to the natural abundance of the raw materials and the ability to use both raw material (polymeric) and the molecular (monomeric) feedstocks in the production of the aerogels [7]. These bio-aerogels are demonstrating potential in further fields of application such as environmental remediation [11]. In contrast, the conversion of proteins into bio-aerogels has received little attention. However, the potential use of proteins as a precursor material for bio-aerogels is of interest due to the (1) abundance of biomass-derived proteins available globally [12], (2) gel-forming characteristics of proteins, and (3) chemical functionality of proteins. Proteins obtained as co-products from food processing are particularly promising sources of raw feedstocks for bio-based materials [13]. Certain polysaccharides are chosen for their functional surface groups (e.g. amino groups on chitosan) [14]; however, the presence of functional groups in amino acids (e.g. thiol, hydroxy, amine, amide and carboxy groups) suggests that proteins may have extended chemical functionality over their polysaccharide counterparts. Indeed, enzymes have been preserved during formation of aerogels, and the resulting aerogels retained the functionality of those enzymes [15]. Functionalising protein aerogels with inorganic particles has also been demonstrated and paves the way for possible applications in bio-catalysis and bio-detection [16]. Similar to polysaccharide aerogels, protein-based aerogels are also candidates for drug or nutrient delivery and are of particular interest as tissue scaffolding materials due to macro-porous morphologies [17]. The inherent gelation capacity of certain proteins [18] facilitates processing of aerogels by removing the need for added crosslinkers. Despite these promising attributes, there are limited examples of protein-based aerogels in the literature, with the bulk of these derived from animal sources (e.g. egg protein [19], milk protein [20], silk [21], and collagen [22, 23]). Reports on the use of plant-derived proteins in aerogels in the literature are scarce (e.g. soy protein) [24].

Bio-aerogels derived from new sources of protein have the potential to broaden the range of precursors and functional properties. Here, proteins extracted from *Brassica napus* canola seed meal (CSM) are used to produce a new range of bio-aerogels via a facile aqueous-based, freeze-drying process. The motivation for extracting proteins from CSM for bio-aerogels is due to their abundance as a co-product of canola oil [25] and tendency for gelation [26]. Cruciferin and napin are known to be the two major protein constituents of extracts from *B. napus* seed meal, and it is known that cruciferin contributes towards gelation in canola protein isolates [25]. Cruciferin is a 300–350-kDa polypeptide with six subunits arranged as two large trimers held together predominantly by non-covalent bonding such as hydrophobic, electrostatic, and hydrogen interactions [27]. These interactions can be modified through extrinsic processing such as pH changes and energy sources to promote intermolecular interactions and subsequent gelation [28]. Proteins have a variety of chemical functional groups including amine groups ($–NH_2$), carboxyl groups (–COOH), hydroxyl groups (–OH), aromatic rings, and sulphhydryl groups (–SH), and these can all participate in protein–protein interactions during gelation. Cruciferin gelation is stabilised by hydrogen bonding and hydrophobic interactions with some contribution from disulphide bridging [29]. Preliminary assessments of the morphological and mechanical properties of the resulting canola protein bio-aerogels are reported to investigate potential applications.

Experimental procedures

Experimental materials

Canola seed meal (CSM) was sourced from *B. napus* (Pure Oil NZ Limited, Rolleston, New Zealand). N-hexane, sodium hydroxide pellets (98.5–100%), hydrochloric acid (36.5–38%), and methanol (99.9%) were obtained from Thermo Fisher Scientific (New Zealand). Tris(hydroxymethyl)aminomethane (Tris), dithiothreitol (DTT), urea, sodium dodecyl sulphate (SDS), acetic acid, ethanol (absolute), ammonium sulphate, and phosphoric acid were obtained from Merck (New Zealand). Bromophenol blue and glycerol were obtained from Bio-strategy (New Zealand). SDS concentrate buffer (0.25 M Tris, 1.92 M glycine, 1% SDS), 4–20% Criterion™ TGX™ precast gel, Coomassie blue stain G250, and Precision Plus Protein™ Standards were obtained from Bio-Rad (New Zealand). All solutions were prepared using reverse osmosis (RO) water (resistivity 18 MΩ) from a Milli-Q water purification system.

Protein extraction

Canola proteins were extracted from CSM using an alkali-acid extraction method adapted from Klockeman et al. [30] Firstly, 250 g of CSM was rinsed in 500 mL of hexane to remove residual oil. After drying, 200 g of the CSM was suspended in 2 L of a 0.4% NaOH solution (at 10% w/v ratio) and agitated for at least 1 h. The solubilised protein was separated from the insoluble fraction using centrifugation at 18520 × *g* for 30 min. The protein extract was then precipitated by the addition of 2 M HCl until a pH of 3.5 was attained. The precipitate was isolated via centrifugation at 18520 × *g* for 30 min, followed by freeze drying.

Sodium dodecyl sulphate polyacrylamide gel electrophoresis (SDS-PAGE)

The recovered protein extract was then analysed by SDS-PAGE using a 4–20% Criterion™ TGX™ precast PA-gel (Bio-Rad) and a 0.025 M Tris, 0.192 M glycine, 0.1% w/v SDS buffer (Bio-Rad). Protein extract samples were solubilised in electrophoresis buffer (6 M urea, 0.062 M Tris, 6% DTT, 10% glycerol, 0.001% bromophenol blue, 2% SDS, pH 6.8) at a concentration of 6.67 mg mL^{-1} and heated in boiling water for 4 min. The electrophoresis tank was prepared with 10 × diluted SDS buffer (final concentration 0.025 M Tris, 0.192 M glycine, 0.1% w/v SDS, pH 8.3) and the PA-gel. Five micro-litres of denatured extract samples was then loaded onto the gel alongside a Precision Plus Protein™ Standards (Bio-Rad) molecular weight marker. Electrophoresis was carried out at 200 V, 0.08 A, 15 W for 45 min. The gel was then immersed in a fixing reagent (10% acetic acid, 40% water, 50% ethanol) for 30 min and then stained using Coomassie Brilliant Blue G-250 solution (16.6% w/v ammonium sulphate, 0.166% w/v Coomassie Brilliant Blue G-250, 16.6% v/v phosphoric acid, 33.3% v/v methanol) overnight and finally destained using RO water and lint-free tissues.

Preparation of bio-aerogels

The dried extract powder was dispersed in Milli-Q water to a final concentration of 10 wt.% (unless otherwise stipulated) and with pH values of 6.0, 7.0, 8.0, 9.0, 9.5, 10.0, 10.5, 11.0, 11.5, and 12.0. The pH of the CSM extract dispersions was adjusted using 2 M NaOH or 2 M HCl solutions. Following adjustment of the pH, a selection of dispersions was also heat-treated in a water bath at temperatures of 60, 70, 80, or 90 °C for 30 min. The aqueous protein dispersions were then mixed until homogenous, followed by brief sonication to remove air bubbles. The homogenous dispersions were then transferred to 15 mL Falcon™ Conical Centrifuge Tubes (15.0 mm Ø (internal)) in approximately 8 mL aliquots per tube and stored at − 80 °C for at least 12 h prior to freeze drying in a Dura-Dry MP manifold dryer (FTS Systems) at 30 to 50 mTorr and room temperature. The resulting aerogels have estimated Brunauer–Emmett–Teller (BET) specific surface areas in the order of 0.8 $m^2 g^{-1}$ based on the measurement of one sample prepared at a pH of 10 and at 25 °C. Low specific surface areas (< 5 $m^2 g^{-1}$) are expected in freeze-dried aerogels [20], and similar results are reported for the BET surface areas of another freeze-dried, protein aerogel (1.7–3 $m^2 g^{-1}$) [31]. Further measurements of BET surface areas in CSM protein aerogels are the focus of ongoing studies.

Materials characterisation

The bulk density of the aerogels was determined from measurements of the volume and mass. Vernier

callipers were used to measure the average diameter and height ($n = 3$) of the cylindrical specimens (± 0.01 mm). A microbalance was used to weigh the aerogel specimens (Mettler Toledo AB204, ± 0.001 g).

The structure of the canola aerogel was imaged using a SkyScan 1172 micro-computed tomography scanner (Bruker-microCT, Kontich, Belgium) at 34 kV and 210 µA producing 2400 images at 15.18-µm resolution. Reconstruction procedures (NRecon version 1.6.10.2 software, Bruker-microCT) produced axial cross sections (Supporting Information) and a 3-dimensional reconstruction of the specimen.

The microstructure of the aerogels was characterised using a Hitachi TM3030 Plus scanning electron microscope (SEM) (magnifications < 2000 ×) and a JEOL JSM 7000F SEM (magnifications > 2000 ×). Specimens were sputter-coated with gold to a thickness of 100 Å (DSR1 Desk Sputter Coater (Nanostructured Coatings Co.)) prior to secondary electron imaging. Specimens were imaged using an accelerating voltage of 15 kV (JSM 7000F) or 5 kV (JSM-IT300). Micro-structural features were quantified by image analysis using Fiji Image J image processing software [32].

Mechanical properties

The mechanical properties of the aerogels were measured in compression using a universal electromechanical testing system (Model 4204, Instron, Norwood USA) equipped with a 100 N load cell. Each batch of aerogels gelled at ambient temperature allowed for the production of 5 monolithic specimens, allowing for the preparation of 10 replicate test specimens for each pH condition. In the case of heat-treated gels, only one viable batch was produced, resulting in one monolith per pH per temperature value which allowed for two specimens in mechanical tests ($n = 2$). Cylindrical specimens (11–13 mm Ø, h = 15–20 mm) were cut from the monoliths using a surgical scalpel blade (Swann-Morton No. 10). Specimens were compression-tested using a constant crosshead speed of 1 mm min^{-1}. Specimens were compressed until the load cell limit was reached (≥ 80% strain). Compressive stress–strain plots were determined from the load–displacement data. The average and standard deviation ($n = 10$ or 2) of the elastic modulus (E) and yield strength (σ_y) of the aerogels were determined.

Results and discussion

CSM protein extract for bio-aerogel manufacture

The quantity of protein extract obtained from the raw CSM was 14% of the total dry weight. This equates to 35% of the available protein in the meal, assuming 40% protein content [27]. A yield of 35% available protein is consistent with use of the alkali-acid extraction technique, where 30% of total protein is typically extracted from one fraction [25]. Multiple repeats of the protein extraction were shown to consistently produce the same bands in SDS-PAGE analysis. The major protein bands of this extract were: 28.5, 25.5, 20.5, 18, 16.5, and 9.5 kDa (Fig. 1). All bands were analysed for protein identification using liquid chromatography–mass spectrometry (LC–MS), and the extract was found to be predominantly composed of cruciferin protein. Ten of the fourteen bands analysed were exclusively composed of cruciferin polypeptides, while three of the remaining bands were largely cruciferin polypeptides (Supporting Information). It is known that cruciferin forms gels more readily, producing stronger gels compared with the other proteins in CSM [33]. The cruciferin content in the extracted proteins was expected to be beneficial for gelation of the extract. Hence, the alkali-acid extraction technique used here appears to be suitable for preparing the CSM as a precursor for synthesis of aerogels.

Processing-structure relationships of CSM-derived protein-based aerogels

Wet-gel processing

The pH of the formulation was critical to the formation of stable gels and subsequent aerogels. Wet gels prepared at a pH of 8 form the most viscous wet gels and gel more rapidly than other pH values at ambient temperatures. Gels prepared with a pH of 8 to 9.5 did not flow upon inversion of the gel given sufficient gelation time. The suspension becomes more transparent and flows upon inversion at a pH greater than 9.5. Low pH values (pH = 3–6) result in the CSM extract powder not completely solubilising, and it does not gel (Fig. 2a). Interestingly, at extremely low pH (pH = 2) the CSM extract appears to be soluble and will form a viable aerogel after freeze drying (not

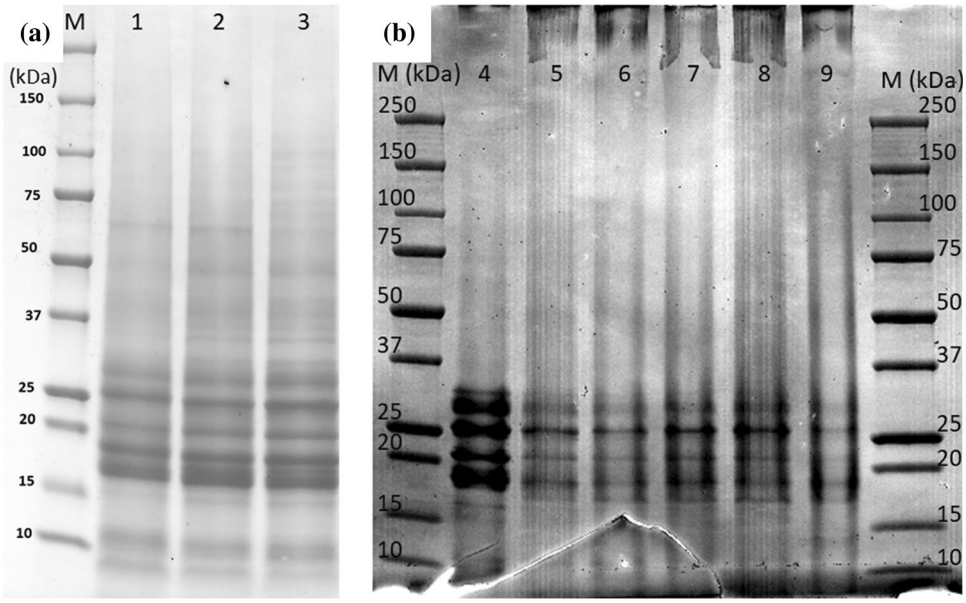

Figure 1 SDS-PAGE analysis of canola seed meal extracts 1–3 (**a**) and 4–9 (**b**) with molecular weight standards from 10 to 250 kDa. Batch numbers are annotated at the top of the corresponding lane, and lanes containing the molecular weight marker are annotated with the letter 'M'.

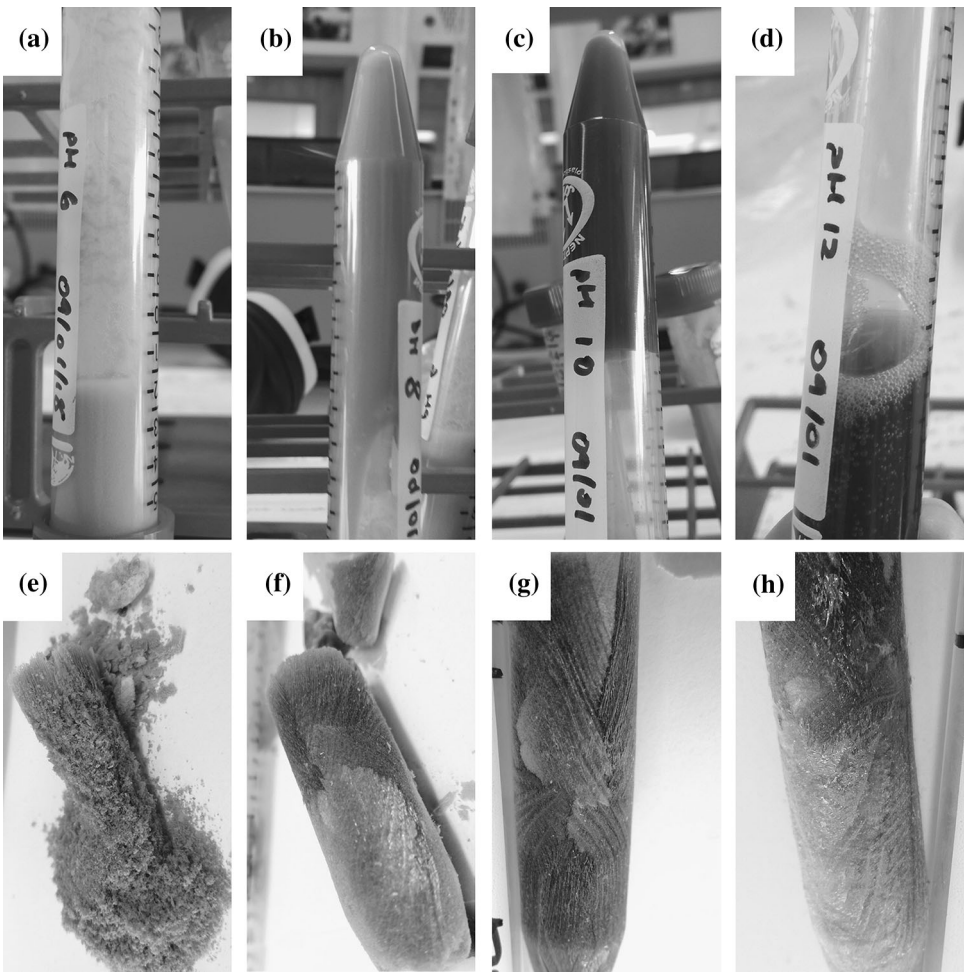

Figure 2 CSM protein extract in water (10 wt.%) (**a**–**d**) and freeze-dried aerogels (**e**–**h**) at pH 6 (**a**, **e**), pH 8 (**b**, **f**), pH 10 (**c**, **g**), and pH 12 (**d**, **h**).

shown). Despite the variable viscosity of the wet gels, all alkaline pH values from 7 and above formed viable aerogel structures once dried. However, suspensions of CSM extract at acidic pH values (3–6),

notably near the isoelectric point (3.5) of the extracts, did not form aerogel monoliths but rather crumbled to powders upon freeze drying (Fig. 2e). The dried CSM gels formed golden-brown monolithic aerogels. The monoliths largely retained the cylindrical and conical shape of the Falcon™ tubes from within which they were formed, although accompanied by ~ 10–20% shrinkage (Fig. 2f–h).

Aerogel microstructure

Generally, the porosity of an aerogel is classified according to pore size (or width) such that macro-pores, meso-pores, and micro-pores are > 50 nm, 2–50 nm, and < 2 nm in width, respectively. The pore morphology is a critical factor that largely determines the suitability of an aerogel in a specific application. For example, the thermal insulation afforded by an aerogel is maximised when the pore size of the aerogel lies in the meso-porous range [34]. Typically, protein-based aerogels have low fractions of meso- or micro-pores, with a tendency for their structures to be dominated by macro-pores, often attributed to freeze drying [20]. Pore morphology of aerogels is governed by both the gelation mechanism and the drying technique used to remove the solvent [7]. CSM protein aerogels examined by X-ray micro-tomography (μ-CT) were also found to mainly exhibit macro-porosity following a freeze-drying processing route (Fig. 3). Interestingly, the porosity observed in the CSM protein aerogels was largely found to be organised in layers of elongated macro-pores that range in width from 30 to 200 μm and from 100 μm to over 3000 μm in length. The layered macro-pores are distinct from the much smaller macro-pores (1–10 μm diameter) and possible meso-pores (< 50 nm) that occur sparsely within the matrix of the aerogel.

Three-dimensional reconstruction of the μ-CT images reveals a value of 52.6% porosity in the entire specimen as calculated from the binarised images at 15-μm resolution. Considering the density of the specimen was 0.12 g cm^{-3} and the theoretical density of a dried, 10 wt.% CSM protein aquagel is 0.10 g cm^{-3}, then the total porosity of the sample is estimated at 88%. The finding of approximately 53% porosity in the μ-CT 3D reconstruction indicates that approximately 35% of the porosity can be found in pores of less than 15 μm in size.

The macro-pores change in shape and size in different locations within the aerogel with the average sample containing macro-pores ranging from 50 μm near the core up to 125 μm in width near the surface (average 75 μm). The macro-pores also demonstrate localised regions of anisotropy (Figs. 3, 4) attributed to unidirectional growth of ice crystals during the freezing process [35]. The walls of the macro-pores range from 1 to 20 μm in thickness with an average of 6 μm. An increase in the density of the aerogel was observed with an increase in protein concentration. Changes in density were also reflected in changes to the layered morphology where the average spacing between macro-pores decreased from 150 to 40 μm with an increase in protein concentration from 3 to 15 wt.% (Fig. 4a–c). Remarkably, changes in the pH did not change the average spacing between the macro-pores (Figs. 4d, 3f). The lack of influence of pH on the aerogel macro-porosity is consistent with the macro-

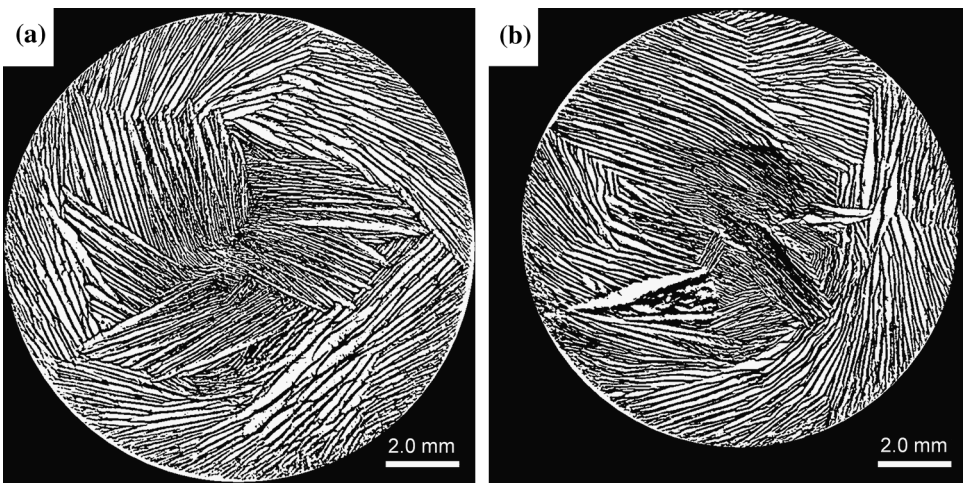

Figure 3 X-Ray micro-tomograms of a CSM protein aerogel (prepared at 10 wt. % and pH = 12) taken at *z*-axis positions of 0.030 mm (**a**) and 15.182 mm (**b**) in a cylindrical specimen (*h* = 30 mm, ø = 12.8 mm).

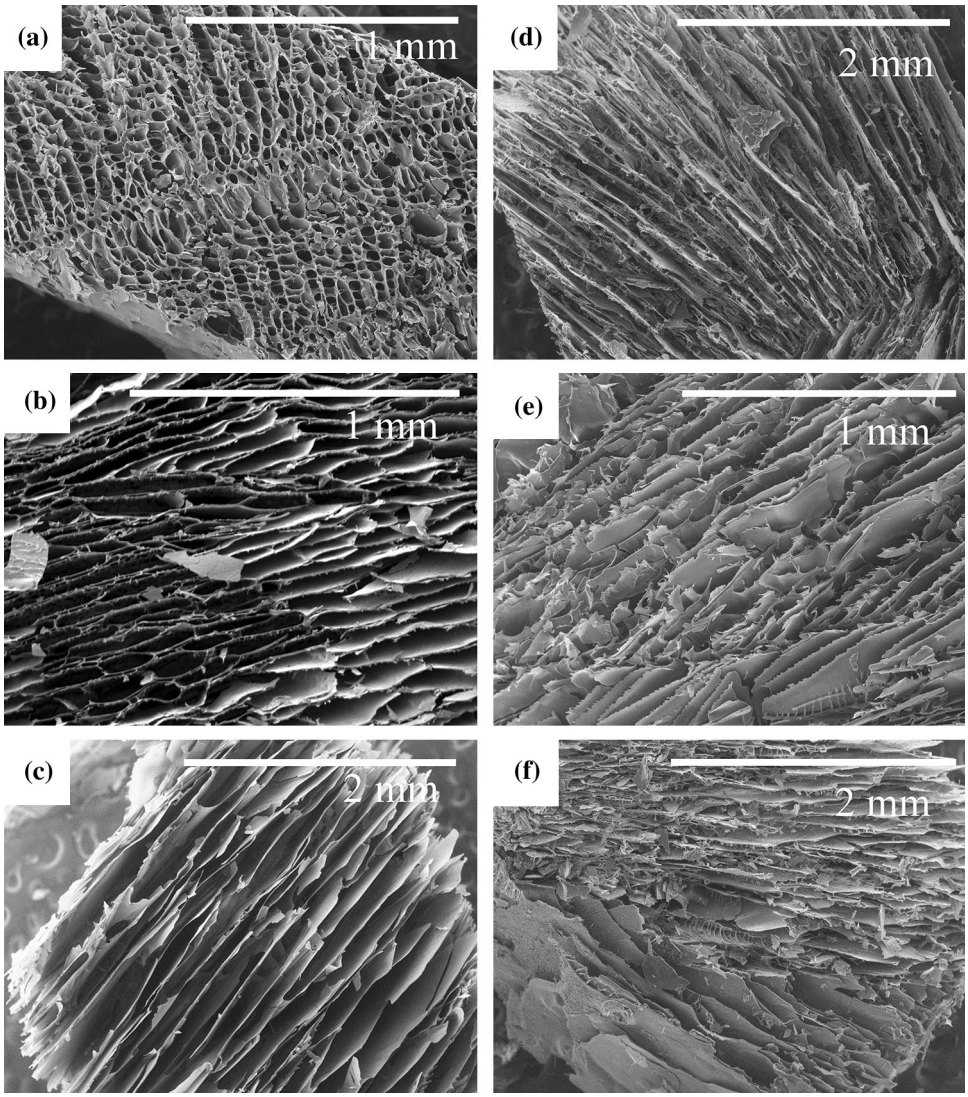

Figure 4 SEM micrographs of CSM protein aerogel morphology as a function of protein concentration (**a**–**c**) and pH (**d**–**f**). Protein concentrations were prepared at 15 wt.% (**a**), 10 wt.% (**b**) and 3 wt.% (**c**) at a pH of 11. Further pH variations were prepared at pH 8 (**d**), pH 10 (**e**), and pH 12 (**f**), at protein concentrations of 10 wt.%.

porosity being largely determined by the freeze-drying process (Figs. 4d, 3f).

Furthermore, varying the pH of the CSM protein aerogels does not appear to alter the presence and size of smaller macro-pores (< 1 μm) or meso-pores (< 50 nm) within the protein matrix across a pH range of 8–11 (Fig. 5).

Another intriguing feature of the aerogel matrix revealed by SEM is the presence of particles on the surface of the otherwise smooth matrix walls (Fig. 6a, b, e–f). These particles on the surface of the aerogel matrices appear to be influenced by the formulation pH of the aerogels. These particles range in diameter from 100 nm to > 1 μm (Fig. 6a, b, e–f) and notably increase in size from a pH of 7 to 8. The average diameter of these particles at pH 7 is 170 nm while at pH 8 they increase to an average diameter of 1.2 μm and then decrease to 600 nm at a pH of 12. The proposed mechanism of CSM protein gelation is a multi-step process of protein denaturation, aggregation, and particle-based network formation. This type of gelation is observed in other globular protein gels such as whey and egg proteins [36]. Denatured protein forms protein aggregates that can form a gel network through further stabilisation and association of protein aggregates [37]. It is possible that the 100–1000-nm-sized particles visible in micrographs may be manifestations of a similar particle-based gelation process in the formation of CSM protein gels. Furthermore, it is known that pH plays a role in protein aggregate sizes in other aerogels [19] and could offer an explanation for these particle size differences with varying pH (Fig. 6b, e–f).

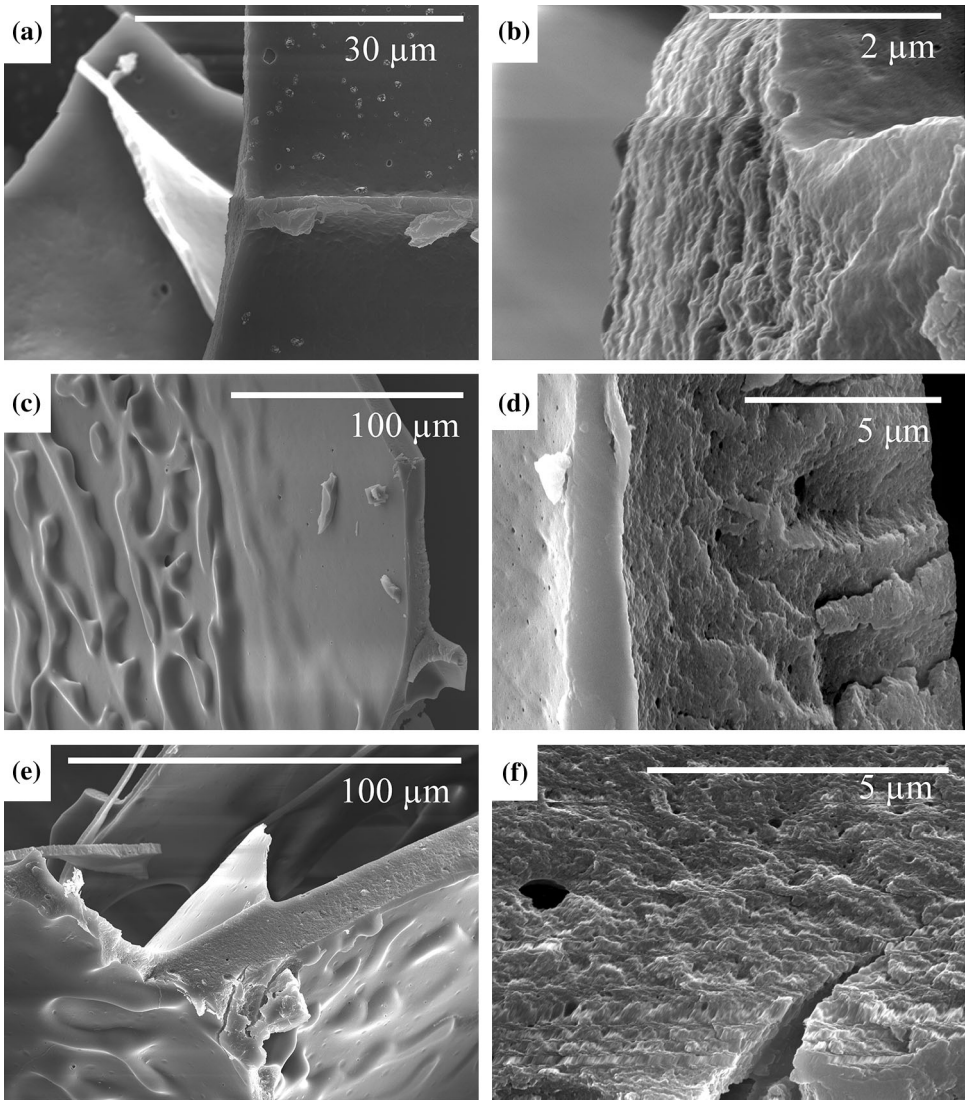

Figure 5 SEM micrographs of CSM protein aerogels at high magnification. Cross sections of aerogel samples prepared at pH 8 (**a**, **b**), pH 9 (**c**, **d**), and pH 11 (**e**, **f**) with protein concentrations of 10 wt.%.

The imaging of particles and pores at the sub-micron scale (Figs. 5, 6) suggests the possibility of meso-pores (< 50 nm in diameter) inside the protein matrix. The macro-pores may result from a meso-porous gel network that is compressed by ice crystal growth during freezing prior to freeze drying. In future work, drying of the CSM gel by super-critical CO_2 extraction of the gel solvent will be used to improve the preservation of the gel structure to further explore meso-porosity formation in these materials. The development of a meso-porous CSM protein aerogel would make these aerogels advantageous for applications where high surface areas combined with biocompatibility and biodegradability are required (e.g. drug delivery). Bio-aerogels have been used in applications that require specific levels of macro-porosity (e.g. cell scaffolding in tissue engineering) [17]. Hence, the macro-porous CSM protein aerogels developed in this work using the freeze-drying route are potential candidates for similar applications.

Compressive mechanical properties of CSM-derived protein-based aerogels

Static compression tests carried out on the cylindrical monolithic aerogels produced typical aerogel stress–strain curves. The elastic linear region is present up to approximately 6% compression. The linear region is followed by a plateau in stress that marks the onset of the compaction phase in aerogel deformation where the gradual collapse of the pore structure begins [38]. The dimensions of the specimen are further distorted during a densification phase at strains greater

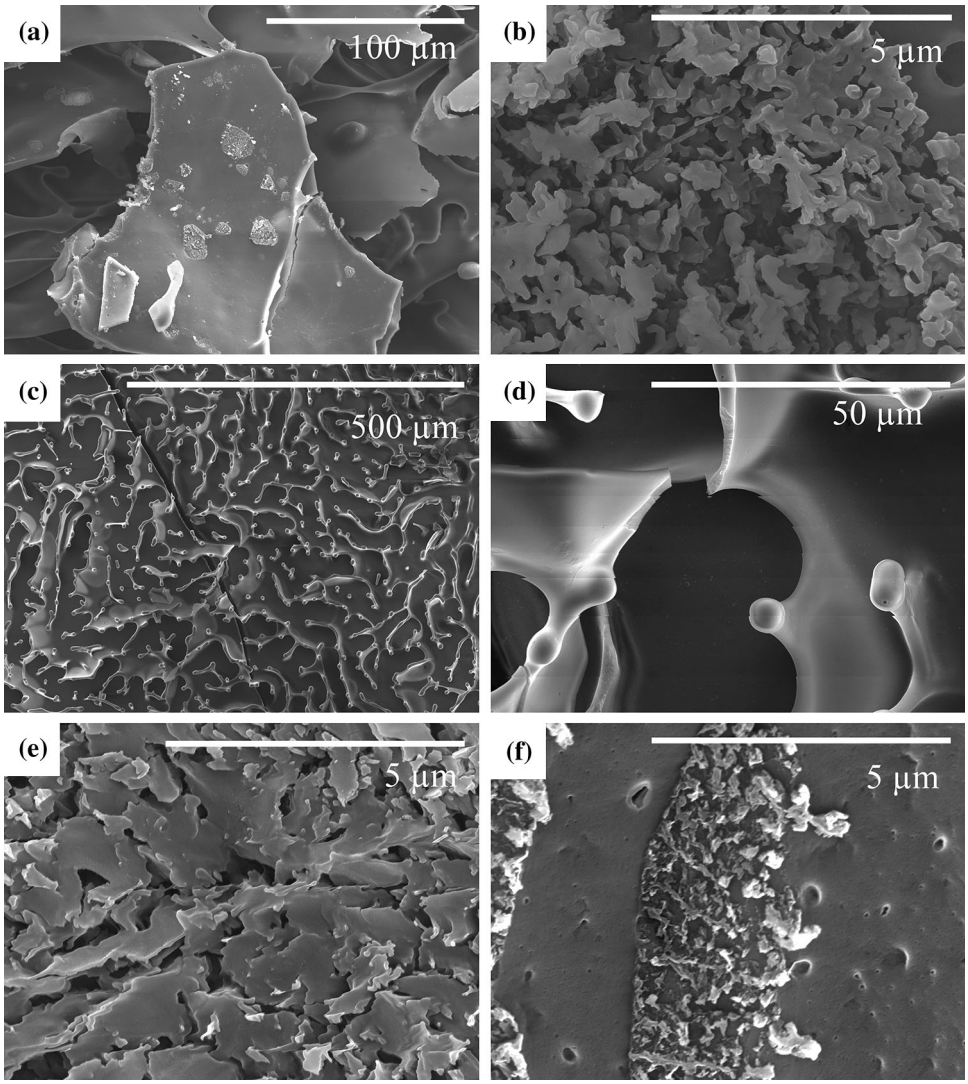

Figure 6 SEM micrographs of morphological features appearing on the surface of CSM protein aerogel matrices. Surface of matrix from CSM protein aerogel prepared at pH 12 (**a**, **b**), pH 10 (**c**, **d**), pH 8 (**e**), and pH 7 (**f**) at 10 wt.% protein concentration.

than ~ 55–60%, as the collapsed pore structure of the aerogel is compressed (Fig. 7). The yield stress of an aerogel is sometimes referred to as the collapse strength and is used for comparison of compressive strength in aerogels [38]. Silica aerogels are well known for their brittle nature and have an onset of the plateau occurring at a compressive strain of ~ 5% [38]. Similarly, CSM protein aerogels exhibit a limited linear elastic region, with the onset of the plateau region occurring at ~ 6% strain.

The elasticity of aerogels is important for applications such as tissue engineering where some exemplary aerogels demonstrate a linear elastic regime up to 60% compression [39]. CSM protein aerogels demonstrate much less elastic deformation at 6%; however, similar values of elasticity are reported for other protein-based examples (e.g. 5% for silk fibroin aerogels prepared at 6 wt.%.) where increased wt.% values tend to reduce the elastic region [17]. Preparation of CSM protein aerogels at lower wt.% concentrations may be one route for improving elasticity and assessing potential for application in tissue engineering applications, as demonstrated in silk fibroin aerogels.

As for other porous media, the mechanical performance of the material is directly correlated to the porosity (or density) of the aerogel [34]. The density of the CSM protein aerogels may be controlled via the concentration of the protein in the wet gel (Fig. 8). The stiffness-to-density and strength-to-density ratios (a.k.a. specific elastic modulus and specific strength, respectively) of porous materials are useful for comparing different materials, particularly where it is desirable to maximise both the mechanical properties

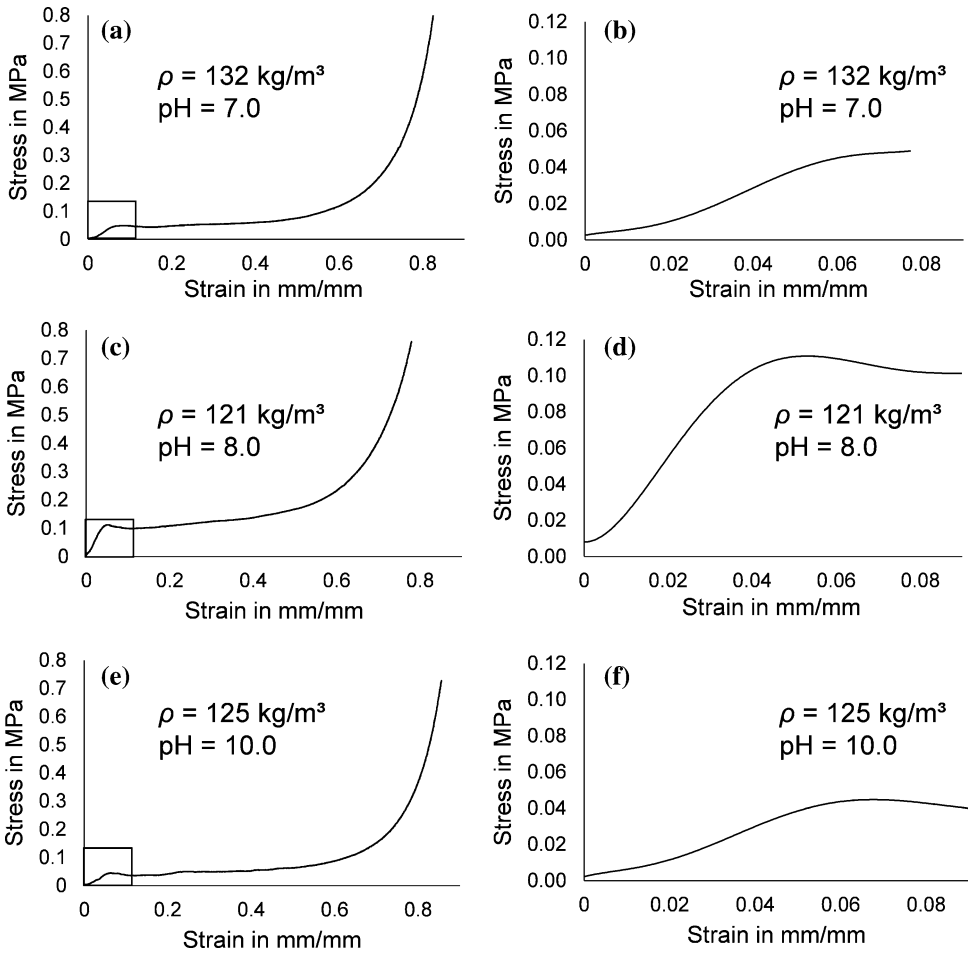

Figure 7 Stress–strain data from compressive tests of CSM protein aerogels prepared at pH 7 (**a**, **b**), pH 8 (**c**, **d**), and pH 10 (**e**, **f**) with a 10 wt.% protein concentration (aerogel densities of 132 kg m^{-3}, 121 kg m^{-3}, and 125 kg m^{-3}, respectively). The linear elastic regions of plots **a**, **c**, and **e** are shown enlarged in plots **b**, **d**, and **f**, respectively.

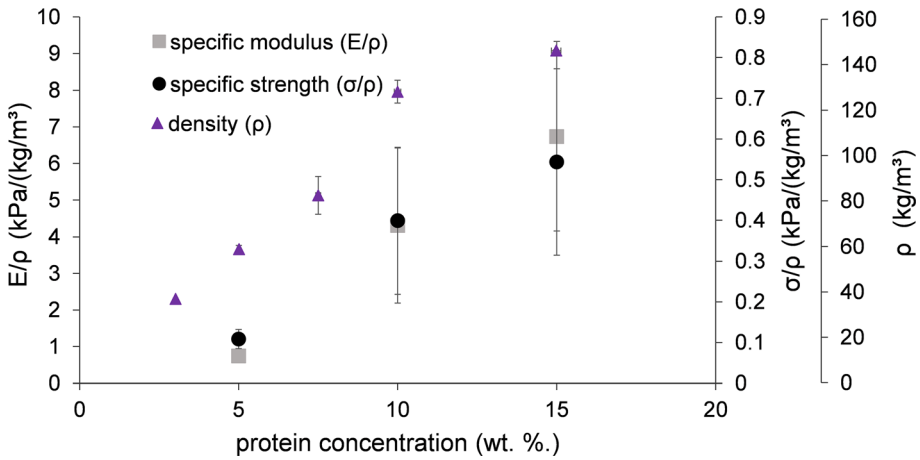

Figure 8 Density and compressive mechanical properties (specific elastic modulus and strength) of CSM protein aerogels as a function of the protein concentration. Error bars represent the standard deviation of measurements where $n = 2$.

and porosity. CSM extract aerogels demonstrate an increase in specific mechanical properties with increasing concentration of protein. The nonlinear dependence of the mechanical properties on density is a characteristic of nearly all biopolymer aerogels as summarised in a recent review by Zhao et al. [7]. The authors summarised mechanical data from a range of studies on biopolymer aerogels and their composites; however, no protein-based aerogels contributed to the studies of compressive modulus (E) dependency on density (ρ). The findings in the present study demonstrate that protein-based aerogels are likely to also have a nonlinear dependence of E on ρ (Fig. 7). Repeated testing may improve the variance observed

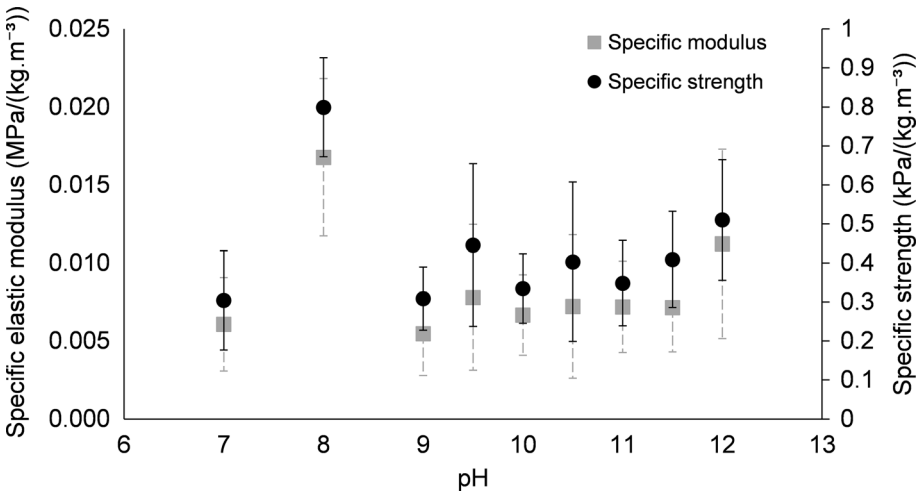

Figure 9 Specific compressive strength and elastic moduli of CSM protein aerogels as a function of pH during formulation. Samples are prepared at 10 wt.% and at ambient temperature. Error bars represent the standard deviation of samples at each pH value where $n = 10$.

in these results (since $n = 2$); however, one explanation for high variance in mechanical data is the observation of macroscopic anisotropy in the aerogels. The control of thermal gradients during the freezing process may allow for production of isotropic CSM protein aerogels and should be investigated as a possible method for reducing variance in CSM protein aerogel properties.

A protein concentration of 10 wt.% was used for subsequent aerogel formulations to ensure that CSM formulation concentration remained comparable with other protein aerogels such as egg white protein [19], whey protein [40], and silk fibroin [41] aerogels. The 10 wt.% CSM aerogels have an average density of 130 kg m^{-3}, although viable aerogels with densities as low as 37 kg m^{-3} could be produced using a protein concentration of 3 wt.%. Aerogels with densities as low as 59 kg m^{-3} were sufficiently stable to be prepared as cylindrical specimens for compressive tests (Fig. 8).

CSM protein aerogels (10 wt.% protein concentration) have an average compressive modulus of 0.97 ± 0.32 MPa and average compressive strength of 0.055 ± 0.011 MPa, respectively (Table 1). Corresponding average values for specific modulus and strength are 0.008 ± 0.003 MPa (kg $m^{-3})^{-1}$ and 0.47 ± 0.25 kPa (kg $m^{-3})^{-1}$, respectively. Additionally, the compressive mechanical properties of the aerogels can be manipulated by altering the pH and temperature of the formulation during gelation. The

Table 1 Comparison of CSM protein aerogel compressive mechanical properties

Aerogel type	Average compressive *E* (MPa)	Average compressive strength (MPa)	Density (kg m^{-3})	Average specific E (MPa (kg $m^{-3})^{-1}$)	Average specific strength (kPa (kg $m^{-3})^{-1}$)
CSM protein aerogels at 10 wt.%[a]	0.97 ± 0.32	0.055 ± 0.011	118 ± 5	0.008 ± 0.003	0.47 ± 0.25
CSM protein aerogel at 10 wt.%, pH 10 and $T = 90$ °C	2.66 ± 0.45	0.134 ± 0.002	114 ± 2	0.023 ± 0.004	1.18 ± 0.04
Whey protein isolate aerogels [40]	18.2	N/A[b]	256	0.071	N/A
Silk fibroin aerogels [41]	3.3	0.32	N/A	N/A	N/A
Clay–soy protein–PVOH aerogels [42]	4.0	0.05	79	0.051	0.6

[a]Averages are calculated from all samples represented in Figs. 8 and 9. Variance is calculated using % standard deviations in contributing data

[b]N/A = data not available

highest elastic modulus and strength achieved in CSM protein aerogels were 2.66 ± 0.45 MPa and 0.134 ± 0.002 MPa, respectively, in a sample prepared at 10 wt.% protein, pH 10.0, and a heat treatment of 90 °C for 30 min during gelation.

The compressive mechanical properties of CSM protein aerogels vary in comparison with other protein aerogels (Table 1). The specific mechanical properties of CSM protein aerogels remain less than those of whey protein aerogels [11% the specific modulus of whey protein aerogels (Table 1)]. However, one specimen (prepared at 90 °C and pH = 10) achieves over twice the stiffness and strength of the average CSM protein aerogels (32% the specific modulus of whey protein aerogels). A comparison to a soy protein composite aerogel shows certain CSM protein aerogels outperform these hybrids in terms of compressive strength [197% the specific strength (Table 1)]. Further comparison to silk fibroin aerogels shows CSM protein remains < 30% the compressive stiffness and strength (Table 1). Whey protein isolate, silk fibroin, and soy protein composite aerogels provide the only comparative data in the literature. The scarcity of comparative data highlights the need for a better understanding of the mechanical capabilities of protein-based aerogels. Here, it must be noted that CSM protein aerogels were prepared from non-fibrous proteins and without the use of crosslinking factors or reinforcing fibres. The comparative data obtained from other studies of protein-based aerogels contain examples of fibrous proteins (silk fibroin) [41], crosslinking factors (whey protein gelled with calcium salts) [40], and hybrid aerogels (clay/soy protein/PVOH) [42] in which these factors play a role in the gelation and strengthening process. Therefore, CSM protein aerogels are a promising addition to this group, demonstrating that they have the potential to achieve comparable or improved mechanical properties with similar gel-enhancing techniques.

Processing-structure–property relationships of CSM protein aerogels

The gelation mechanism likely involves a combination of hydrophobic interactions, hydrogen bonding, ionic bonds, and disulphide covalent bonding [27]. Many of these molecular interactions are influenced by the pH and by other charged species present in solution (i.e. salt ions). CSM protein wet gels are known to have pH- and temperature-dependent rheological properties, where alkaline pH and a temperature above 82 °C are optimal for gel network formation [27]. Thus, it is expected that the aerogels in this study would follow a similar trend and have mechanical properties dependent on these same gelation parameters. Aerogels prepared using varying alkaline pH values (pH 7–12) and gelation temperatures (25–90 °C) were tested for their compressive mechanical behaviour.

Compressive mechanical testing demonstrates that gels prepared with a pH of 8 have superior mechanical properties to other pH preparations, with an elastic modulus of 2.0 ± 0.6 MPa (specific modulus of 0.017 ± 0.005 MPa (kg $m^{-3})^{-1}$) and compressive strength of 96 ± 14 kPa (specific strength of 0.80 ± 0.13 kPa (kg $m^{-3})^{-1}$) (Fig. 9). In contrast, the aerogels prepared at pH 7 or pH 9 do not exceed moduli of 0.7 MPa or strengths of 40 kPa, suggesting that a pH at or near 8 plays a role in the gel strength of these CSM aerogels. Another observation of mechanical testing is a slight tendency for increased strength and stiffness with increasing pH in the samples from pH 9–12.

The influence of aerogel morphological features (i.e. porosity) on gel strength can be investigated by analysis of the morphology alongside the mechanical data. Analysis of structural features from Figs. 3, 4 and 5 showed no effect of varying alkaline pH on the macro-porosity or matrix cross section. A lack of morphological differences of the macrostructure of the aerogels with changes in pH suggests that differences in mechanical properties are related to the finer details of the structure (e.g. protein aggregate size) or molecular interactions (e.g. degree of crosslinking). Generally, the pH of a protein gel influences gel strength in a protein-specific manner since the isoelectric point (pI) of protein differs between protein types [28]. Gelation can occur at a pH near pI when non-charged protein aggregates form a particle-based network such as in soy protein isolates [37]. However, a pH distant to pI can also favour gelation when extreme pH is necessary for protein denaturation, prior to gelation. Canola protein isolate is known to produce stronger wet gels at high pH (9.0), distant to the pI of the isolate (pI = 5.6), and this is attributed to the role of an alkaline environment in the denaturation of the canola protein [37]. A similar dependence of canola protein gelation on alkaline pH is observed in this study, where the protein pI is estimated between 3.5 and 5.0 based on

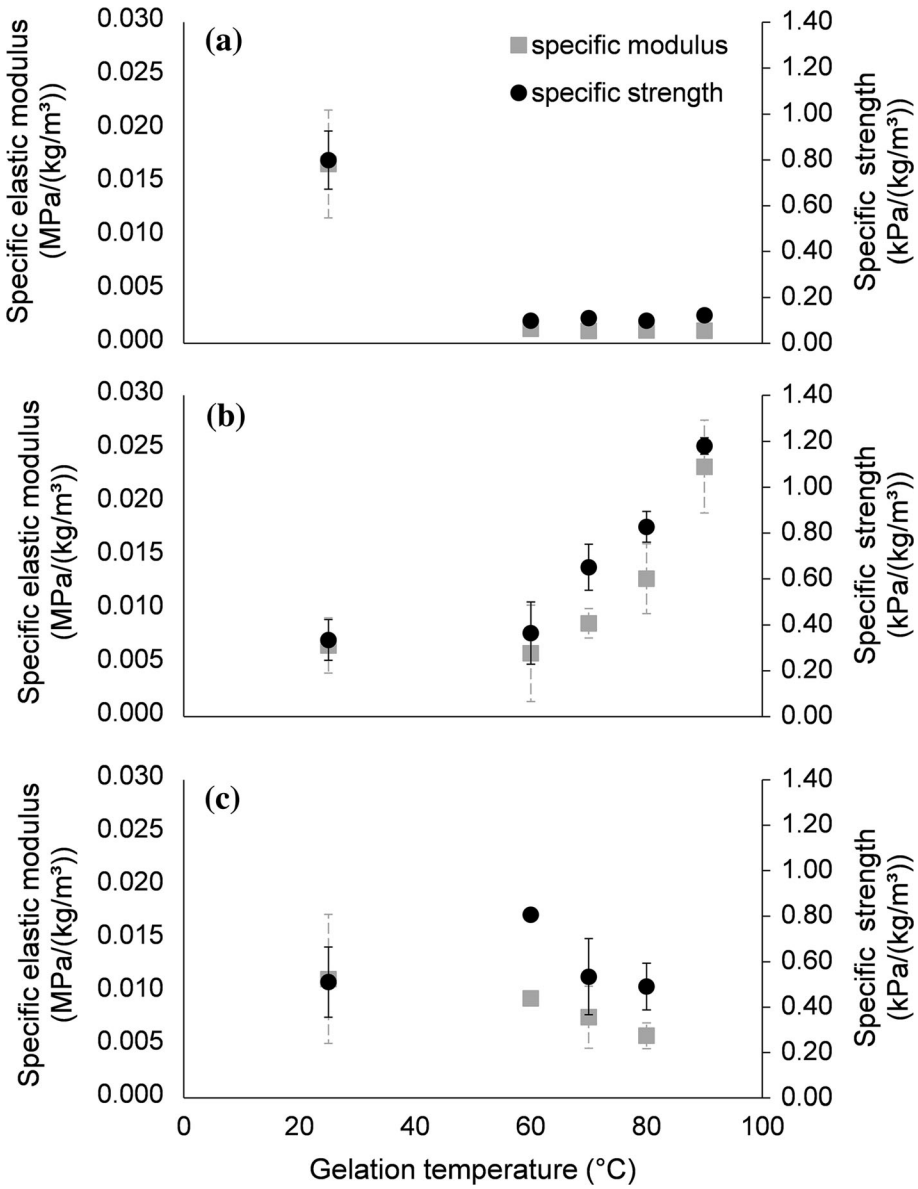

Figure 10 Specific compressive mechanical properties of CSM protein aerogels as a function of temperature prepared at pH 8 (**a**), pH 10 (**b**), and pH 12 (**c**). Error bars represent the standard deviation of measurements where $n = 10$ at 25 °C and $n = 2$ at all other temperatures. The specimen prepared at pH 12 and a temperature of 60 °C allowed for only one measurement; therefore, no statistical information is available.

the precipitation point during protein extraction. One explanation for the reduction in gel strength beyond pH 8 is the increasing influence of repulsive negative charges to protein aggregates that reduce the association of protein molecules during gel formation. Future studies of the sol–gel precursors of CSM protein aerogels will elucidate the relationship between pH-induced protein denaturation, protein aggregation, and resulting gel and aerogel strengths. Additionally, preparation of CSM protein aerogels by super-critical fluid extraction may better preserve the wet-gel structures and possibly allow for pH-induced morphological differences in wet gels to be observed in the final aerogels.

CSM aerogels samples were also prepared at various gelation temperatures and subsequently tested for mechanical properties (Fig. 10). Interestingly, formulations based on a pH of 10 appear to be influenced by changes in gelation temperature (25–90 °C), while formulations based on a pH of 8 or 12 are not. The highest compressive mechanical properties are seen in pH 10 samples prepared with gelation temperature of 90 °C (specific compressive modulus 0.022 ± 0.004 MPa $(\text{kg m}^{-3})^{-1}$ and specific compressive strength 1.18 ± 0.04 kPa $(\text{kg m}^{-3})^{-1}$). The samples at pH 10 increase in strength and stiffness with increasing temperature; however, this contrasts with the pH 12 samples which do not

experience changes in strength and stiffness with changes in gelation temperature. These results indicate that the effect of pH and temperature on the mechanical strength of the aerogels is a complex interaction of factors which requires further elucidation.

The combined influences of pH and temperature demonstrate the tuneability of the CSM protein aerogels using simple aqueous techniques, allowing for preservation of biodegradability which can be lost when chemical crosslinkers such as aldehydes are used to improve mechanical performance of materials. While the specific strengths and stiffnesses of protein aerogels remain below those of most polysaccharide-based aerogels [7], a certain advantage in some applications may be afforded to protein-based bio-aerogels for their unique biochemical properties and tuneable processing, e.g. the controlled release of an absorbed bioactive compound during digestion.

Conclusions

Aerogels were made from canola seed meal (CSM) protein using pH-controlled gelation and a freeze-drying process. The aerogels have a layered, macroporous morphology with an average density of 0.13 g cm^{-3} at 10 wt.% protein concentration. The presence of some meso-porosity suggests that a homogenous, meso-porous structure may be obtainable via alternate drying techniques such as supercritical fluid extraction with appropriate solvents.

The average compressive modulus of CSM protein aerogels is 0.97 ± 0.32 MPa, and the average compressive strength is 0.055 ± 0.011 MPa although some CSM protein aerogels can achieve moduli up to 2.66 MPa and compressive strengths of up to 0.134 MPa. Mechanical properties of CSM protein aerogels are comparable with other protein-based aerogels in the literature, including those with fibrous or crosslinked proteins.

Compressive mechanical properties can be altered through manipulation of the pH, protein concentration, and temperature during the gelation process, revealing the tunability of aerogel properties by aqueous chemical methods. The CSM protein gel is likely formed from association of pH-sensitive protein aggregates (100–1000 nm diameter) to produce gel networks which are then partially conserved through freeze drying.

Given that the CSM protein aerogels are bio-based, these bio-aerogels are candidates for current bio-aerogel applications such as drug delivery, cell scaffolding, and in food science.

Supporting Information

Supporting Information is available from the Wiley Online Library or from the author.

Acknowledgements

The authors would like to thank Biopolymer Network Limited (New Zealand) for supporting this research programme and associated doctoral stipend. Additionally, this research was also made possible through technical support from staff in the Proteins and Biomaterials team at AgResearch Limited (New Zealand).

Compliance with ethical standards

Conflicts of interest The authors declare that there are no conflicts of interest.

Electronic supplementary material: The online version of this article (https://doi.org/10.1007/s10853-019-04330-w) contains supplementary material, which is available to authorized users.

References

[1] Akimov YK (2003) Fields of application of aerogels (review). Instrum Exp Tech 46(3):287–299

[2] Hüsing N, Schubert U (1998) Aerogels—airy materials: chemistry, structure, and properties. Angew Chem Int Edition 37(1–2):22–45

[3] Dorcheh AS, Abbasi M (2008) Silica aerogel; synthesis, properties and characterization. J Mater Process Technol 199(1):10–26

[4] Leventis N, Lu H (2011) Polymer-crosslinked aerogels. In: Aegerter MA, Leventis N, Koebel MM (eds) Aerogels handbook. Springer, New York, pp 251–285

[5] Pierre AC (2011) History of Aerogels. In: Aegerter MA, Leventis N, Koebel MM (eds) Aerogels handbook. Springer, New York, pp 3–18

[6] Pierre AC, Pajonk GM (2002) Chemistry of aerogels and their applications. Chem Rev 102(11):4243–4266

[7] Zhao S, Malfait WJ, Guerrero-Alburquerque N, Koebel MM, Nyström G (2018) Biopolymer aerogels and foams: chemistry, properties, and applications. Angew Chem Int Edition 57(26):7580–7608

[8] Stergar J, Maver U (2016) Review of aerogel-based materials in biomedical applications. J Sol-Gel Sci Technol 77(3):738–752

[9] Ulker Z, Erkey C (2014) An emerging platform for drug delivery: aerogel based systems. J Control Release 177:51–63

[10] Kleemann C, Selmer I, Smirnova I, Kulozik U (2018) Tailor made protein based aerogel particles from egg white protein, whey protein isolate and sodium caseinate: influence of the preceding hydrogel characteristics. Food Hydrocolloids 83:365–374

[11] Yang W-J, Yuen ACY, Li A, Lin B, Chen TBY, Yang W, Lu H-D, Yeoh GH (2019) Recent progress in bio-based aerogel absorbents for oil/water separation. Cellulose 26(11):6449–6476

[12] Fitzpatrick SE, Staiger MP, Deb-Choudhury S, Ranford S (2018) Chapter 6 protein-based aerogels: processing and morphology. In: Biobased aerogels: polysaccharide and protein-based materials. The Royal Society of Chemistry, pp 67–102

[13] Shi W, Dumont M-J (2014) Review: bio-based films from zein, keratin, pea, and rapeseed protein feedstocks. J Mater Sci 49(5):1915–1930. https://doi.org/10.1007/s10853-013-7933-1

[14] Ricci A, Bernardi L, Gioia C, Vierucci S, Robitzer M, Quignard F (2010) Chitosan aerogel: a recyclable, heterogeneous organocatalyst for the asymmetric direct aldol reaction in water. Chem Commun 46(34):6288–6290

[15] Li YK, Chou MJ, Wu TY, Jinn TR, Chen-Yang YW (2008) A novel method for preparing a protein-encapsulated bioaerogel: using a red fluorescent protein as a model. Acta Biomater 4(3):725–732

[16] Nyström G, Fernández-Ronco MP, Bolisetty S, Mazzotti M, Mezzenga R (2016) Amyloid Templated Gold Aerogels. Adv Mater 28(3):472–478

[17] Mallepally RR, Marin MA, Surampudi V, Subia B, Rao RR, Kundu SC, McHugh MA (2015) Silk fibroin aerogels: potential scaffolds for tissue engineering applications. Biomed Mater 10(3):035002

[18] Doi E (1993) Gels and gelling of globular proteins. Trends Food Sci Technol 4(1):1–5

[19] Selmer I, Kleemann C, Kulozik U, Heinrich S, Smirnova I (2015) Development of egg white protein aerogels as new matrix material for microencapsulation in food. J Supercrit Fluids 106:42–49

[20] Betz M, García-González CA, Subrahmanyam RP, Smirnova I, Kulozik U (2012) Preparation of novel whey protein-based aerogels as drug carriers for life science applications. J Supercrit Fluids 72:111–119

[21] Baldino L, Cardea S, Reverchon E (2016) Loaded silk fibroin aerogel production by supercritical gel drying process for nanomedicine applications. Chem Eng Trans 49:343–348

[22] Lu T, Li Q, Chen W, Yu H (2014) Composite aerogels based on dialdehyde nanocellulose and collagen for potential applications as wound dressing and tissue engineering scaffold. Compos Sci Technol 94:132–138

[23] Jiang J, Zhang Q, Zhan X, Chen F (2019) A multifunctional gelatin-based aerogel with superior pollutants adsorption, oil/water separation and photocatalytic properties. Chem Eng J 358:1539–1551

[24] Amaral-Labat G, Grishechko L, Szczurek A, Fierro V, Pizzi A, Kuznetsov B, Celzard A (2012) Highly mesoporous organic aerogels derived from soy and tannin. Green Chem 14(11):3099–3106

[25] Aider M, Barbana C (2011) Canola proteins: composition, extraction, functional properties, bioactivity, applications as a food ingredient and allergenicity—a practical and critical review. Trends Food Sci Technol 22(1):21–39

[26] Léger LW, Arntfield SD (1993) Thermal gelation of the 12S canola globulin. J Am Oil Chem Soc 70(9):853–861

[27] Wanasundara JP, McIntosh TC, Perera SP, Withana-Gamage TS, Mitra P (2016) Canola/rapeseed protein-functionality and nutrition. OCL 23(4):D407

[28] Totosaus A, Montejano JG, Salazar JA, Guerrero I (2002) A review of physical and chemical protein-gel induction. Int J Food Sci Technol 37(6):589–601

[29] Kim JH, Varankovich NV, Stone AK, Nickerson MT (2016) Nature of protein-protein interactions during the gelation of canola protein isolate networks. Food Res Int 89:408–414

[30] Klockeman DM, Toledo R, Sims KA (1997) Isolation and characterization of defatted canola meal protein. J Agric Food Chem 45(10):3867–3870

[31] Ahmadi M, Madadlou A, Sabouri AA (2015) Isolation of micro- and nano-crystalline cellulose particles and fabrication of crystalline particles-loaded whey protein cold-set gel. Food Chem 174:97–103

[32] Schindelin J, Arganda-Carreras I, Frise E, Kaynig V, Longair M, Pietzsch T, Preibisch S, Rueden C, Saalfeld S, Schmid B, Tinevez J-Y, White DJ, Hartenstein V, Eliceiri K, Tomancak P, Cardona A (2012) Fiji: an open-source platform for biological-image analysis. Nat Methods 9(7):676–682

[33] Tan SH, Mailer RJ, Blanchard CL, Agboola SO (2011) Canola proteins for human consumption: extraction, profile, and functional properties. J Food Sci 76(1):R16–R28

[34] Aegerter MA, Leventis N, Koebel MM (2011) Aerogels handbook. Springer, Berlin
[35] Zhang X, Liu M, Wang H, Yan N, Cai Z, Yu Y (2019) Ultralight, hydrophobic, anisotropic bamboo-derived cellulose nanofibrils aerogels with excellent shape recovery via freeze-casting. Carbohydr Polym 208:232–240
[36] Alting AC, Hamer RJ, De Kruif CG, Visschers RW (2003) Cold-set globular protein gels: interactions, structure and rheology as a function of protein concentration. J Agric Food Chem 51(10):3150–3156
[37] Kim JHJ, Varankovich NV, Nickerson MT (2016) The effect of pH on the gelling behaviour of canola and soy protein isolates. Food Res Int 81:31–38
[38] Lu H, Luo H, Leventis N (2011) Mechanical characterization of aerogels. In: Aegerter MA, Leventis N, Koebel MM (eds) Aerogels Handbook. Springer, New York, pp 499–535
[39] Si Y, Yu J, Tang X, Ge J, Ding B (2014) Ultralight nanofibre-assembled cellular aerogels with superelasticity and multifunctionality. Nat Commun 5(1):5802
[40] Chen HB, Wang YZ, Schiraldi DA (2013) Foam-like materials based on whey protein isolate. Eur Polym J 49(10):3387–3391
[41] Kim U-J, Park J, Li C, Jin H-J, Valluzzi R, Kaplan DL (2004) Structure and properties of silk hydrogels. Biomacromol 5(3):786–792
[42] Finlay K, Gawryla MD, Schiraldi DA (2008) Biologically based fiber-reinforced/clay aerogel composites. Ind Eng Chem Res 47(3):615–619